

# STATUS OF THE DUAL-AXIS RADIOGRAPHIC HYDROTEST FACILITY

M.J. Burns, P.W. Allison, R.L. Carlson, J.N. Downing, D.C. Moir, and R.P. Shurter  
Los Alamos National Laboratory, P.O. Box 1663, Los Alamos, NM 87545

## Abstract

The Dual-Axis Radiographic Hydrodynamics Test (DARHT) Facility will employ two electron Linear Induction Accelerators to produce intense, bremsstrahlung x-ray pulses for flash radiography with sub-millimeter spatial resolution of very dense (attenuations  $> 10^5$ ), dynamic objects. We will produce an intense x-ray pulse using a 19.75-MeV, 3.5-4 kA, 60-ns flattop electron beam focused onto a tungsten target. A 3.75-MeV injector with either a cold velvet cathode or a laser-driven photocathode will produce a beam to be accelerated through a series of 64 ferrite-loaded induction cells with solenoid focusing. Accelerator technology demonstrations have been underway for several years at the DARHT Integrated Test Stand (ITS) and results including beam energy, emittance, and Beam Break-Up (BBU) measurements are discussed here.

## I. Introduction

To meet DARHT mission requirements we must produce a large x-ray dose ( $\sim 1000$  Roentgen one meter from the source) in short bursts ( $< 100$ -ns) from a very small source size ( $\sim 1.2$ -mm equivalent diameter of a uniformly illuminated disk at 50% modulation). Detailed considerations of detector response, test object transmission and scatter, and the bremsstrahlung spectrum limit maximum electron beam energy to  $\sim 20$ -30-MeV. With this energy limit, the high dose and short pulse width specifications require high peak current because dose is related to total charge on the target and beam energy. The small source size requires the electron beam to be focused to  $\sim 1$ -mm diameter, thus requiring very good beam quality. Therefore, we have selected a Linear Induction Accelerator (LIA) for DARHT. This paper summarizes the principal accelerator systems installed on the Integrated Test Stand (ITS), which is the initial 5.75-MeV section of the first DARHT accelerator. Photoelectric cathode development, ITS electron-beam measurements, and facility construction status are also discussed.

## II. Integrated Test Stand (ITS)

The ITS is shown in Fig. 1. It was first operated in 1991 with the purpose of developing and demonstrating the LIA advances required to meet DARHT performance specifications [1]. Over 30,000 pulses have been accumulated on the ITS, including the experiments reported here.

The relatively long, pulsed-power injector consists of a prime power supply that pulse-charges a glycol Blumlein that, in turn, discharges into a series of three transmission lines with impedance changes to step-up the voltage driving the diode [2]. The prime power source consists of a 3.0- $\mu$ F capacitor bank charged to  $\sim 120$ -kV dc, and switched through the primary of a 1:15 Stangenes iron-core auto-transformer by a single air-blown spark gap. The glycol Blumlein consists of a 7.65- inner line and a 7.3- outer line and is pulse-charged to 1.5-MV in 4.6- $\mu$ s. The Blumlein is switched with four,

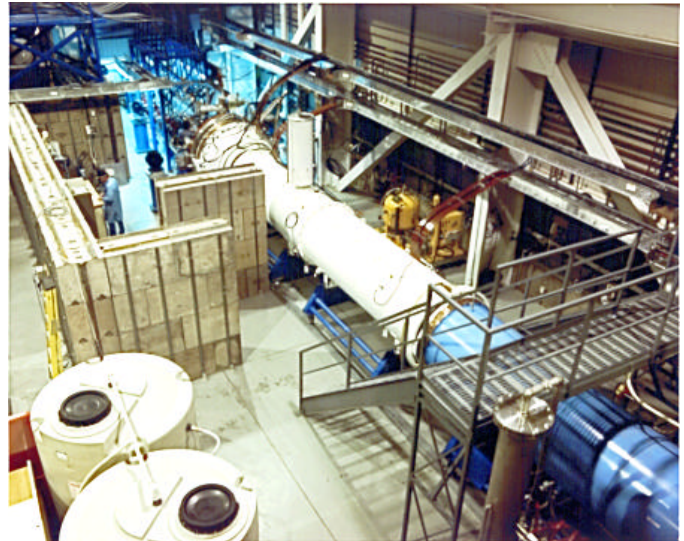


Fig 1. The ITS (injector in the foreground and cell-block beyond)

parallel, laser-triggered spark gaps (measured 1- jitter of 0.7-ns). The Blumlein contains an adjustable peaker and L-C filter, which shapes the initially sharp-rising pulse to a  $[1 - \cos(\pi t)]$  shape with a 10-90% risetime of 20-ns. Three transmission lines in series transform the pulse from 1.5-MV to a maximum of 4-MV on the diode.

The vacuum diode consists of a 170- liquid resistor load in parallel with the 181-mm A-K gap. Our typical 90-mm diameter velvet emitter is inset approximately 2-mm into the cathode field-forming electrode and produces 4-kA at 3.75-MeV. The radial vacuum insulator is cross-linked polystyrene (REXOLITE 1722), 1.8-m in diameter and 0.35-m thick, with capacitive grading provided by the liquid resistor forming a radial wedge in parallel with six concentric aluminum grading rings embedded in the insulator. Although the injector insulator can operate up to 4-MeV, we typically run at 3.75-MeV to minimize emission from our cathode shroud.

The accelerator induction cells [3] for the ITS are assembled into an eight-cell "cell-block". Completion of the first DARHT LIA requires seven additional cell-blocks. Each cell has a 148.2-mm-diam. bore, 19.1-mm accelerating gap, 11 oil-insulated TDK PE16B nickel-iron-zinc ferrite toroids (237-mm ID, 503-mm OD, 25.4-mm thick), a low-dielectric constant ( $\sim 2.5$ ) cross-linked polystyrene insulator, a quadrifilar-wound solenoid magnet with iron homogenizer rings [4], two cosine-wound dipole trim-magnets (to compensate for possible installation tilts of the solenoid magnet), and a cosine-wound quadrupole magnet.

Calculations of the magnetic field caused by pulsed-power currents fed into the cell via two radial lines located on either side of the cell showed a quadrupole field with an estimated gradient-length product of  $\sim 3$ -Gauss. The presence of the field was experimentally confirmed by observation of an asymmetric beam distribution downstream of the cell-block. Cosine-wound quadrupole magnets installed within the cell around the beamtube immediately downstream of each feedline

pair has eliminated the beam asymmetry that leads to emittance growth and a larger effective radiographic source size.

The Induction Cell Pulsed Power (ICPP) consists of four water-insulated, 11- Blumleins with coaxial midplane-triggered switches operating in SF<sub>6</sub> [2]. A single Blumlein is connected to two accelerator cells via four, Dielectric Sciences 2158, 44- cables. Each Blumlein has a separate charging unit which uses two 1.4- $\mu$ F Maxwell primary capacitors charged to 29-kV. Two EEV CX-1722 thyratrons are used in parallel to switch the capacitors into a 1:11 Stangenes iron-core step-up transformer that charges the Blumlein to 250-kV in 5- $\mu$ s. The Blumleins provide a 250-kV, 67-ns pulse to the cells with a 0.6%-rms variation over the beam pulse-width of 60-ns. Jitter (1  $\sigma$ ) in the coaxial switches ranges from 0.8-1.2-ns over 1000 shots. Each Blumlein has an independent trigger unit housed in a separate oil-insulated steel enclosure that consists of two 30-nF, 70-kV primary capacitors switched by a EEV CX 1725 thyatron into a Stangenes 1:4 step-up auto-transformer that drives a magnetic pulse-compressor which reduces the risetime of the required 200-kV trigger pulse to less than 10-ns into the trigger cable. This in turn results in a risetime of 20-ns at the Blumlein spark gap trigger electrode. Typical trigger system jitter is <275-ps (1  $\sigma$ ) for any consecutive 100 shots.

### III. Photoelectric cathode

We are investigating a photoelectric cathode as an alternative to our present velvet cathode to produce a lower emittance beam so that we may be less sensitive to possible emittance growth through the accelerator and have the possibility for a smaller radiographic source size. Due to the plastic insulators in our accelerator, we must operate the photoelectric cathode at vacuums of 10<sup>-5</sup>-10<sup>-6</sup> Torr, thus prohibiting the use of alkali-metal compounds. We have recently reported on an electron-beam-pumped laser operating at ArF (193-nm) or KrF (248-nm) producing 3.5-J in 100-ns (35-MW) that has been used to illuminate a micro-machined aluminum cathode [5]. On a machine similar to the ITS injector we performed experiments at 2.75-MeV. Quantum efficiency was measured for ArF on micro-machined aluminum at 1x10<sup>-3</sup>. Current densities of 100 A/cm<sup>2</sup> and total currents of 2-kA have been achieved. Beam temperature measurements are underway.

We have also reported recently on characterization of aluminum photocathodes as a function of temperature [6]. In our photocathode test stand an ArF laser is used to illuminate small-scale samples of candidate cathode materials that can be radiatively heated to 200C. A 92% transparent tungsten wire mesh anode is located across a 6.7-mm A-K gap operating at 30-kV dc. We observe a factor of ~2.5 increase in emitted current density for a micro-machined aluminum cathode when it is heated to 150C, indicating the possibility of extracting a 4-kA beam with less than a joule of incident ArF energy. A beam temperature measurement using a heated cathode will be completed to investigate cathode heating effects on beam quality. Using this same test stand we have also begun characterization of polycrystalline (predominantly <1,1,0>), boron-doped, hydrogen-terminated synthetic diamond films which may exhibit quantum efficiencies of ~1%.

## IV. Recent ITS electron beam experiments

### A. Emittance

To determine the emittance and the rms values of beam radius,  $r$ , and  $dr/dz$ , at the A-K gap, we measure the beam radius at  $z=1600$ -mm as a function of current in the anode magnet, centered at 537-mm (cathode location is  $z=0$ ). The light from an OTR foil is captured with a 20-ns gated camera and the distribution is analyzed as a function of time and then fit with our envelope code known as "XTR" to extract the beam parameters in the A-K gap. XTR includes beam-potential depression, diamagnetic-field enhancement, and other high-current effects.

We tested our experiment by imposing an axial field of 65-Gauss on the cathode, which imparts angular momentum to the beam resulting in  $r_{rms} = eBR^2/2mc = 0.233$  cm-rad for a cold, uniform-density beam with  $R=35$ -mm. The XTR-deduced result was 0.23 cm-rad. Without the imposed field, we estimate roughly 10% accuracy and determine  $r_{n,4rms} = 0.15$  cm-rad for our 4-kA, 3.75-MeV beam. This is adequately low to produce a spot radius on the target < 0.5-mm.

### B. Measurement of Beam Break-Up (BBU)

Amplification of transverse beam motion in the accelerating gaps (BBU) must be sufficiently small to prevent smearing of the final focus spot as this would result in increased x-ray source size. We measured the transverse impedance of several different accelerating gaps [7] before choosing our final design. Our input beam has been measured to have low noise (< 20- $\mu$ m displacement) near the dominant accelerating cell resonant frequency of 740-MHz. BBU calculations with a magnetic field varying from ~1.0-2.7 kGauss show that a 4-kA beam can be accelerated to 19.75-MeV with <10% spot size smearing.

We have measured BBU amplification as a function of frequency between 700-to-900-MHz by exciting beam oscillations (typically 0.1-mm) with a tunable rectangular box that was shock-excited by the beam. The amplitudes of the transverse motion were measured before and after the eight ITS cells for both horizontal and vertical orientation of the box. The gains were found to agree approximately with the code predictions with a transport magnetic field lower than nominal so as to not effectively damp the BBU motion (Fig. 2). The best agreements for the inferred cell transverse coupling impedance was within 20% of the measurements in ref. 7.

We have since observed that our beam produces a steady-state quadrupole magnetic field with an integrated gradient-length product of 30-Gauss when passing through the box. The response of the beam position monitors to the resulting elliptical beam is then significantly non-linear to centroid displacements. We are now repeating the BBU measurements with cosine-wound quadrupole magnets near the box. Also, we have connected a ~25-W external rf drive to the box to improve the reproducibility of the initial deflections.

### C. Energy spread

We measure time-resolved beam energy distribution in a single pulse using a 60-degree spectrometer magnet to image a collimated portion of the center of the beam onto a Bicron 422 scintillator viewed with a streak camera. Fig. 3 shows a representative trace from the spectrometer measuring the beam extracted from the ITS injector. The beam has an energy of 3.783-MeV with an rms spread of 0.55%, or  $\pm 1\%$  peak-to-peak, over 60-ns at this point. Tapering of the first injector transmission line and adjustments to the peaking section within the Blumlein will be used to flatten the large central bulge within this trace.

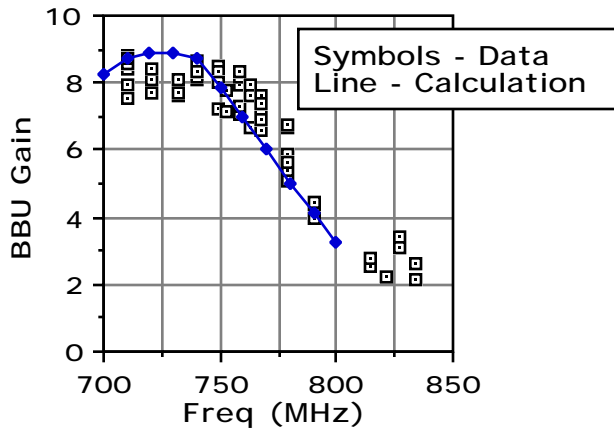


Fig 2 Measured & calculated BBU gain thru ITS cell-block

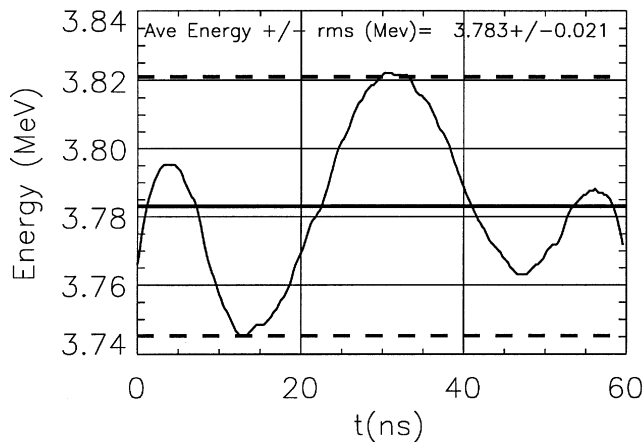


Fig. 3 Injector energy spread with expanded scale

### V. Facility construction status

Fig. 4 shows an artist's rendition of the completed facility, showing two long halls for perpendicular accelerator installation with pulsed-power halls running alongside. Building construction is 30% complete with an estimated finish date of November 1997. The first radiographic experiments are scheduled for June 1999. Operation of the complete, dual-axis facility is expected by September 2001 and is paced by completion of the second accelerator. Prior to construction of the final machine, we will consider designs to deliver four sequential pulses with  $\sim$ MHZ repetition rate.

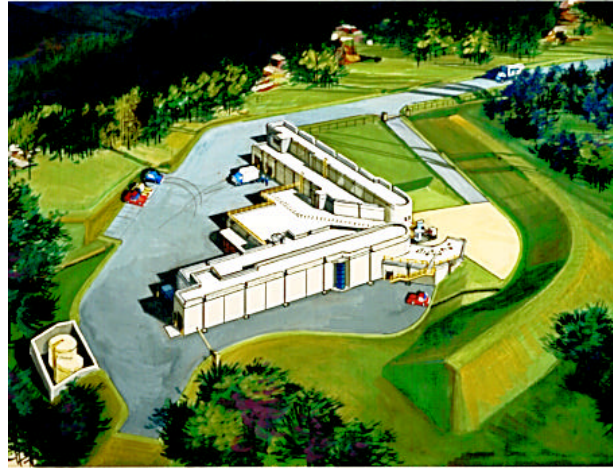


Fig. 4 Artist's rendition of DARHT

### Conclusions

Our work since 1991 indicates that we will achieve the radiographic performance required by DARHT. The principal accelerator components have been tested on the ITS accumulating over 30,000 pulses. Measured beam characteristics have been well-predicted by our computational models and these have been extensively benchmarked and improved against ITS data. An alternative photocathode system is under development to generate a colder beam than our present velvet cathode, thus making us less sensitive to emittance growth and presenting the possibility of achieving a smaller radiographic source size.

### Acknowledgments

Work performed under the auspices of the US Dept. of Energy.

### References

- [1] MJ Burns, et al, "Technology Demonstration for the DARHT Linear Induction Accelerators", *Proceedings of the 9th Intl. Conf. on High-Power Part. Beams*, Washington DC, May 1992
- [2] JN Downing, et al, "Pulsed Power Systems for the DARHT Accelerators", *IEEE 1991 Part. Accel. Conf.*, San Francisco CA, May 1991
- [3] MJ Burns, et al, "Cell Design for the DARHT Linear Induction Accelerators", *IEEE 1991 Part. Accel. Conf.*, San Francisco CA, May 1991
- [4] MJ Burns, et al, "Magnet Design for the DARHT Linear Induction Accelerators", *IEEE 1991 Part. Accel. Conf.*, San Francisco CA, May 1991
- [5] RL Carlson, et al, "Multi-Kiloampere Electron-Beam Generation Using Metal Photo-Cathodes Driven by ArF and KrF Lasers", *Proc. 11th Intl. Conf. on High-Power Part. Beams*, Prague, June 1996
- [6] RP Shurter, et al, "Characterization of Diamond Film and Bare Metal Photocathodes as a Function of Temperature and Surface Preparation", *Proc. 11th Intl. Conf. on High-Power Part. Beams*, Prague, June 1996
- [7] L. Walling, et al, "Transverse Impedance Measurements of Prototype Cavities for DARHT", *IEEE 1991 Part. Accel. Conf.*, San Francisco CA, May 1991